Endogenous nonneuronal modulators of synaptic transmission control cortical slow oscillations in vivo

Tommaso Fellin[a,b,1], Michael M. Halassa[a], Miho Terunuma[a,c], Francesca Succol[a,b], Hajime Takano[a], Marcos Frank[a], Stephen J. Moss[a,c], and Philip G. Haydon[a,c]

[a]Silvio Conte Center for Integration at the Tripartite Synapse, Department of Neuroscience, University of Pennsylvania School of Medicine, Philadelphia, PA 19104; [b]Department of Neuroscience and Brain Technologies, Italian Institute of Technology, 16163 Genova, Italy; and [c]Department of Neuroscience, Tufts University School of Medicine, 136 Harrison Avenue, Boston, MA 02111

Edited by Tullio Pozzan, University of Padua, Padua, Italy, and approved July 14, 2009 (received for review June 10, 2009)

Gliotransmission, the release of molecules from astrocytes, regulates neuronal excitability and synaptic transmission in situ. Whether this process affects neuronal network activity in vivo is not known. Using a combination of astrocyte-specific molecular genetics, with in vivo electrophysiology and pharmacology, we determined that gliotransmission modulates cortical slow oscillations, a rhythm characterizing nonrapid eye movement sleep. Inhibition of gliotransmission by the expression of a dominant negative SNARE domain in astrocytes affected cortical slow oscillations, reducing the duration of neuronal depolarizations and causing prolonged hyperpolarizations. These network effects result from the astrocytic modulation of intracortical synaptic transmission at two sites: a hypofunction of postsynaptic NMDA receptors, and by reducing extracellular adenosine, a loss of tonic A1 receptor-mediated inhibition. These results demonstrate that rhythmic brain activity is generated by the coordinated action of the neuronal and glial networks.

adenosine | astrocytes | gliotransmission | NMDA receptor

Nonrapid eye movement (NREM) sleep is characterized by global cortical oscillations of synchronized neuronal activity (1, 2). Major components of this activity are slow oscillations (<1 Hz), observed also under some forms of anesthesia (2–5). Slow oscillations are a fundamental network phenomenon that organizes other sleep rhythms (1), and have been suggested to have a role in sleep-dependent memory consolidation (6, 7).

Different mechanisms have been proposed to control slow oscillations, including excitatory-inhibitory interactions (8), neuronal intrinsic properties (9, 10), and the modulation of synaptic transmission (4, 11). Although pharmacological (4, 11) studies have shown the importance of synaptic modulation on slow oscillations, it is not known whether endogenous cellular systems capable of modulating synaptic transmission have a role in shaping this cortical rhythm.

Recently, brain slice experiments showed that a glial cell subtype, the astrocyte, modulates synaptic transmission through the release of different molecules (gliotransmission) including D-serine and ATP (12, 13). D-serine acts as a coagonist of NMDA receptors (14) increasing postsynaptic NMDA currents (15), whereas ATP is rapidly hydrolyzed to adenosine, which acts on A1 receptors to suppress synaptic transmission (16, 17). Because astrocytes are intimately associated with pre and postsynaptic terminals (18, 19), on which they exert modulatory actions, they have the potential to act as endogenous regulators of slow oscillations.

Support of this hypothesis comes from the observation that gliotransmission is essential for the normal accumulation of the homeostatic sleep pressure (20). This fundamental process is assessed by measuring the dynamic change in slow wave activity (SWA; 0.5–4 Hz) of the EEG during NREM sleep. Because slow oscillations underlie low frequency (<1 Hz) components of SWA, we hypothesized that gliotransmission may directly impact brain dynamics in the slow oscillation (<1 Hz) range. To test this hypothesis, we have used a combination of glial-cell specific molecular genetics, which inhibits the release of chemical transmitters from astrocytes, together with patch-clamp, extracellular and EEG recordings in vivo to monitor the impact of gliotransmission on the generation of slow oscillations.

We show that the attenuation of gliotransmission leads to reduced cortical slow oscillations. These changes in network activity are due to integrated effects of gliotransmission on A1 and NMDA receptors. These data provide a demonstration that the output of a neuronal network relies on the coordinated activity of an electrically excitable neuronal system in concert with an electrically inexcitable glial cell system, in which synaptic connectivity generates the rhythm that is tuned by glial-dependent neuromodulation.

Results

To determine the role of astrocytes in the regulation of cortical slow oscillations, we used a line of transgenic mice with impaired gliotransmission (17), in which expression of the dominant negative (dn)SNARE domain within astrocytes blocks the release of neuroactive molecules (21), including ATP (17) from these cells. Dominant negative SNARE mice are obtained by crossing two different mouse lines: GFAP.tTA, in which the expression of the tet-off tetracycline transactivator is driven by the astrocyte-specific promoter GFAP, and tetO.dnSNARE, in which the dnSNARE domain of the vesicle protein synaptobrevin II, as well as the reporter EGFP are coexpressed (20) under the control of a tetO promoter (17). Doxycycline (dox) suppresses transgene expression in dnSNARE mice (Fig. S1*A*). To prevent potential developmental influences of transgenes, animals were maintained on a dox-containg diet until weaning, which prevents transgene expression throughout development (20). Dox was then removed for at least 3 weeks (see *Materials and Methods*), and transgene expression was assessed by monitoring the fluorescence of the reporter transgene EGFP (Fig. S1*A*, the use of an antibody against GFP did not result in the staining of additional cells compared with monitoring EGFP fluorescence; Fig. S1*K*). Transgenes were selectively expressed in astrocytes, because EGFP colocalizes with the astrocytic markers GFAP (Fig. S1 *B* and *E*), glutamine synthetase (Fig. S1 *C* and *E*), S100β (Fig. S1 *D* and *E*), but not with the neuronal marker NeuN (Fig. S1 *F* and *J*) nor with NG2, aspartocyclase (ASPA) (22) or Iba1, markers of NG2-positive glia, oligodendrocytes, and microglia, respectively (Fig. S1 *G–J*). GFAP staining is similar in WT and dnSNARE animals (Fig. S1 *L* and *M*),

Author contributions: T.F., M.M.H., and P.G.H. designed research; T.F., M.M.H., M.T., and F.S. performed research; M.F. and S.J.M. contributed new reagents/analytic tools; T.F., M.M.H., M.T., and H.T. analyzed data; and T.F., M.M.H., and P.G.H. wrote the paper.

The authors declare no conflict of interest.

This article is a PNAS Direct Submission.

[1]To whom correspondence should be addressed. E-mail: tommaso.fellin@iit.it.

This article contains supporting information online at www.pnas.org/cgi/content/full/0906419106/DCSupplemental.

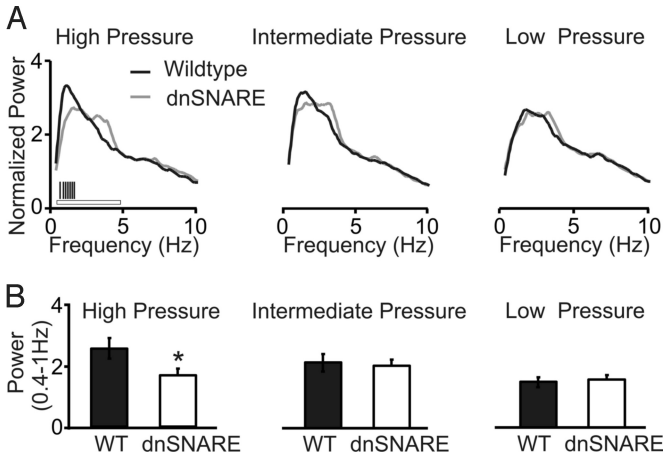

Fig. 1. Dominant negative SNARE animals exhibit reduced EEG low-frequency (<1 Hz) component under conditions of high homeostatic sleep pressure. (*A*) Data were collected from both dnSNARE and WT littermates during NREM sleep (20), and normalized to the total power of the EEG between 0.39–20 Hz (see *Materials and Methods*). High homeostatic pressure corresponds to recovery after sleep deprivation (WT, $n = 7$; dnSNARE, $n = 6$, white horizontal bar: ANOVA, genotype, $F = 5.398$, $P < 0.02$; genotype X frequency, $F = 2.58$, $P < 0.001$, vertical black bars: posthoc test, $P < 0.05$). Intermediate homeostatic pressure corresponds to sleep at the beginning of the light phase (WT, $n = 9$; dnSNARE, $n = 8$, ANOVA, NS). Low pressure corresponds to sleep at the end of the light phase (WT, $n = 9$; dnSNARE, $n = 8$, ANOVA, NS). (*B*) Histograms reporting the average power of the slow oscillations (0.4–1 Hz) in WT and dnSNARE animals under conditions of high sleep pressure (WT, $n = 7$; dnSNARE, $n = 6$) (*Left*), intermediate sleep pressure (WT, $n = 9$; dnSNARE, $n = 8$) (*Center*), and low sleep pressure (WT, $n = 9$; dnSNARE, $n = 8$) (*Right*). *, $P < 0.05$.

suggesting that transgenes expression in astrocytes does not induce reactive astrocytosis.

Dominant Negative SNARE Expression Reduces Slow Oscillations Under Conditions of High Sleep Pressure. Initially, we obtained chronic EEG recordings from freely behaving WT and dnSNARE mice (20) while varying the homeostatic sleep pressure load across the sleep–wake cycle. The self-normalized NREM power spectra of dnSNARE and WT mice were compared at the end of the light-phase (low sleep pressure), at the beginning of the light phase (intermediate sleep pressure), and after sleep deprivation (high-sleep pressure) (see *Materials and Methods*). Dominant negative SNARE mice exhibited a significant reduction in the power within the frequency domain of slow oscillations (0.4–1.0 Hz) under conditions of high homeostatic sleep pressure (Fig. 1).

Gliotransmission Modulates Cortical Slow Oscillations. To investigate the cellular and molecular mechanisms through which gliotransmission modulates brain dynamics in the slow frequency range (<1 Hz), we used anesthetized mice, a preparation that enhances slow oscillations (2, 4). This experimental manipulation further allows single and multiple neurons electrophysiological recordings, as well as local pharmacological manipulations. Because our surface EEG electrodes were mostly recording from cortical areas, we studied cortical slow oscillations, and used this rhythm as a model to understand the role of astrocytes in the modulation of brain activity at the circuit level.

We performed extracellular local field potential (LFP) recordings in vivo from the somatosensory cortex of urethane anesthetized dnSNARE animals and WT littermates. Attenuation of gliotransmission in transgenic animals significantly decreased the power of this rhythm (WT, $n = 37$ animals; dnSNARE, $n = 45$; Fig. 2 *A–C*). Importantly, when dnSNARE expression is prevented by constantly feeding animals with dox, cortical slow oscillation power was undistinguishable from WT littermates similarly fed dox (WT on dox, 0.4-to 1-Hz power, 0.55 ± 0.02, $n = 10$; dnSNARE on dox, 0.54 ± 0.03, $n = 6$, $P > 0.05$).

We confirmed this finding by performing in vivo patch-clamp recordings from pyramidal neurons (Fig. S2*A*) in the somatosensory cortex of WT and dnSNARE animals. Neurons from dnSNARE animals have a significantly lower probability of being at the depolarized potential (up-state probability) compared with controls (Fig. 2 *D* and *E*), whereas the maximal amplitude of the depolarization (up-state amplitude) is similar (Fig. 2*F*). No differences in neuronal input resistance and resting potential were observed between dnSNARE and WT animals (Table S1). Also, up-state transitions occur at lower frequency in dnSNARE animals compared with controls (Fig. 2*G*). The average single cell firing rates were not significantly reduced in dnSNARE mice (control, 0.25 ± 0.11 AP/s, $n = 8$; dnSNARE, 0.06 ± 0.03 AP/s, $n = 9$; $P > 0.05$).

On average, the duration of the depolarized potential (up-state duration) is significantly shorter in dnSNARE animals compared with controls (average values: WT, 0.72 ± 0.02 s, $n = 418$ events from eight mice; dnSNARE, 0.56 ± 0.02 s, $n = 425$ from nine mice; $P < 0.001$ Kolmogorov–Smirnov test) (Fig. S3), and the down-state duration is significantly longer (average WT, 0.82 ± 0.04 s, $n = 427$ from eight mice; dnSNARE, 1.54 ± 0.12, $n = 439$ from nine mice; $P < 0.001$ Kolmogorov–Smirnov test) (Fig. S3). The decreased up-state probability observed in the dnSNARE animals (Fig. 2 *D* and *E*) is, thus, due to shorter and less frequent transitions to the depolarized up state, and longer transitions to the down state (Fig. S3).

Dominant Negative SNARE Expression Does Not Affect Astrocytic Supportive Functions. Because dnSNARE expression inhibits gliotransmission (17, 21), and because of the importance of astrocytes in the homeostatic regulation of the extracellular concentration of K^+ and glutamate, it is necessary to determine whether dnSNARE expression alters astrocytic homeostatic properties. To test this hypothesis, we performed whole-cell recordings from astrocytes in hippocampal slices from both control and dnSNARE animals, and found the glia from these animals to be indistinguishable. Astrocytes exhibited highly negative resting potentials, an absence of action potential firing on depolarizing current injection (Fig. S4 *A* and *B*), a linear I-V relationship, and low input resistance typical of passive astrocytes (Fig. S4 *C* and *D*) (23). No significant differences were observed between astrocytes from control and dnSNARE animals. To assess glial responses to neuronal activity, we evoked synaptic transmission while recording the current responses of astrocytes. These currents are mainly mediated by K^+ channels and glutamate transporters, and can be taken as a measure of the capacity of astrocytes to buffer extracellular K^+ and clear synaptically-released glutamate (24, 25). No differences in current responses of astrocytes were found between control and dnSNARE mice (Fig. S4*E*). Also, the total and surface expression of EAAT2, a major glutamate transporter expressed primarily in astrocytes, is not affected in dnSNARE animals when compared with controls (Fig. S4 *F* and *G*). These data show that expression of the dnSNARE transgene does not alter astrocytic supportive functions, and allow for the conclusion that attenuated cortical slow oscillations in dnSNARE mice does not result from defects in transmitter clearance and K^+ uptake.

Astrocytic dnSNARE Expression Leads to Hypofunction of Neuronal NMDA Receptors. Two main targets of gliotransmission are the A1 adenosine receptor (17) and the NMDA receptor (15, 26). Given that previous studies have shown that the prolonged depolarization phase of the slow oscillations is in part due to the activity of the NMDA receptor (4, 11), we asked whether the decreased

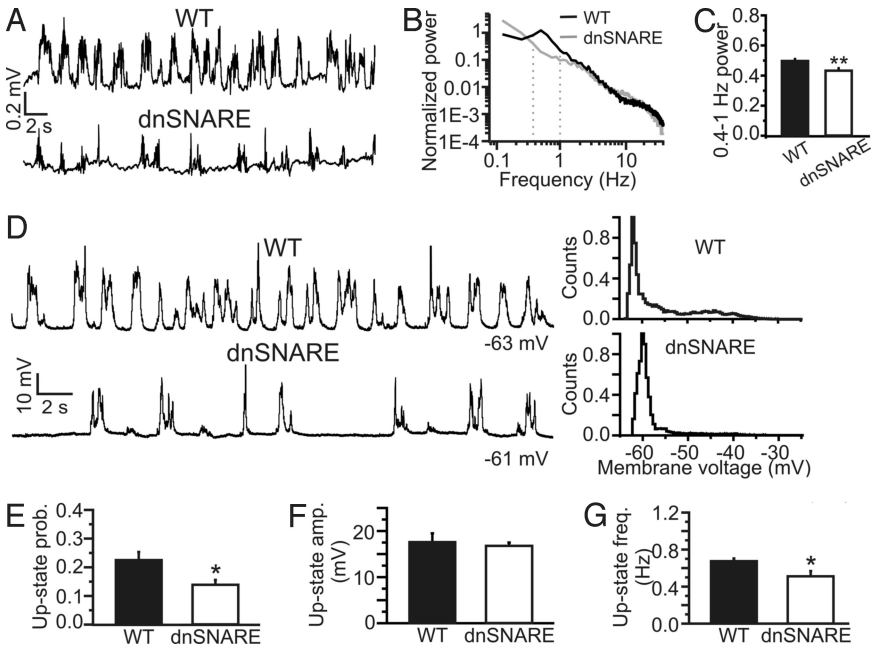

Fig. 2. Reduced slow oscillations in the somatosensory cortex of anesthetized dnSNARE animals. (*A*) Representative LFP recording showing slow oscillation activity in the somatosensory cortex of WT (*Upper*) and dnSNARE (*Lower*) animals. (*B*) Normalized power spectra corresponding to the experiments shown on the left from WT and dnSNARE animals. Power spectra are normalized to the total spectral power (see *SI Materials and Methods*). (*C*) Average power of the slow oscillations (0.4–1 Hz) in 37 WT, 45 dnSNARE animals. Data are shown as percentage of the total spectral power. Student's *t* test was used for evaluating statistical significance. Unless otherwise stated, in this as well as in the other figures: *, $P < 0.05$; **, $P < 0.01$. (*D*) (*Left*) In vivo current-clamp recordings from representative neurons showing slow oscillations in the cortex of WT (*Upper*) and dnSNARE (*Lower*) animals. Action potentials are truncated for presentation purposes. (*Right*) Membrane voltage histogram corresponding to the traces shown on *Left*. (*E*) Average up-state probability. Data are obtained from 11 cells from 8 WT and 14 cells from 9 transgenic animals. When multiple cells were recorded in the same animal, a single value of the up-state probability corresponding to that particular animal was calculated by averaging the values from the different cells. (*F*) Average maximal up-state amplitude in 8 WT and 9 dnSNARE animals. (*G*) Average up-state frequency in WT ($n = 8$) and dnSNARE ($n = 9$) animals.

up-state duration that we observed in the dnSNARE animals could be due to an effect mediated through the NMDA receptors. To test this hypothesis, we first measured, in slice preparations, the AMPA/NMDA current ratio at cortical synapses, which are considered to be essential for the generation of slow oscillations (2, 8, 27, 28).

We performed patch-clamp recordings from layer 2/3 pyramidal neurons (Fig. S2 *C* and *D*) while extracellularly stimulating layer 4, and found the AMPA/NMDA current ratio to be significantly increased in slices from dnSNARE compared with control animals (Fig. 3 *A* and *B*). The increase we observed in AMPA/NMDA ratio could be due to an increase in AMPA receptor activity or to a decrease of NMDA receptor function. To discriminate between these two possibilities, we performed Western blottings, and demonstrated that glial dnSNARE expression did not alter the total protein expression of the AMPA receptor subunits GluR1, GluR2, or the NMDA receptor subunits NR1, NR2A, and NR2B (Fig. 3 *C* and *D*; Fig. S4 *H* and *I*). Immunostaining against the GluR1 and NR2A subunit confirms that the general pattern of distribution of AMPA and NMDA receptors is not altered in dnSNARE mice (Fig. S5). However, surface biotinylation studies to label receptors inserted in the plasma membrane show that astrocytic dnSNARE expression regulated NMDA receptors and selectively reduced NR2A and NR2B, but not NR1, GluR1, and GluR2, subunit surface expression (Fig. 3 *C* and *D*; Fig. S4 *H* and *I*). Given that NMDA receptors require both NR1 and NR2 subunits to form a functional channel, a decrease in the surface expression of the NR2 subunits results in a reduced activity of the receptor.

Because astrocytes exhibit SNARE-dependent D-serine release (29), which potentiates NMDA receptor channel opening (15), we asked whether, in addition to reducing surface NMDA receptor density, dnSNARE expression caused an additional D-serine-dependent reduction in NMDA receptor activity. Application of D-serine (100 μM) did not significantly change the synaptic AMPA/NMDA current ratio of control slices, whereas it led to a small, but significantly increase in the NMDA component of the synaptic current and as a consequence to a decrease in the AMPA/NMDA ratio in slices from dnSNARE mice (Fig. 3 *E–H*). Although this result suggests that cortical astrocytes can normally control NMDA receptor activity by releasing D-serine, it must be noted that addition of exogenous D-serine to slices from dnSNARE animals only partially rescue the AMPA/NMDA ratio to that measured in control slices (Fig. 3 *G* and *H*). This result agrees with the biochemical data, demonstrating that dnSNARE expression leads to a hypofunction of NMDA receptors mainly through a reduction in surface expression of NR2 subunits.

Nonneuronal Regulation of NMDA Receptors Modulates Slow Oscillations. To ask whether astrocyte-dependent changes in NMDA receptor function underlie the alterations in network activity in dnSNARE mice, we performed in vivo pharmacological experiments targeting these receptors in control and dnSNARE animals while monitoring spontaneous activity with LFP recordings. In control experiments, we first determined that there was no significant rundown of cortical slow oscillations during the extended period required to perform pharmacology in vivo (Fig. S6 *A* and *B*), and that topical application on the surface of the brain results in drug diffusion through all of the cortical layers underneath the craniotomy (Fig. S6 *C–E*). Local application of the NMDA receptor antagonist D-(−)-2-amino-5-phosphonopentanoic acid (D-AP5; 50–100 μM) to the cortical surface led to a significant reduction in the power of cortical slow oscilla-

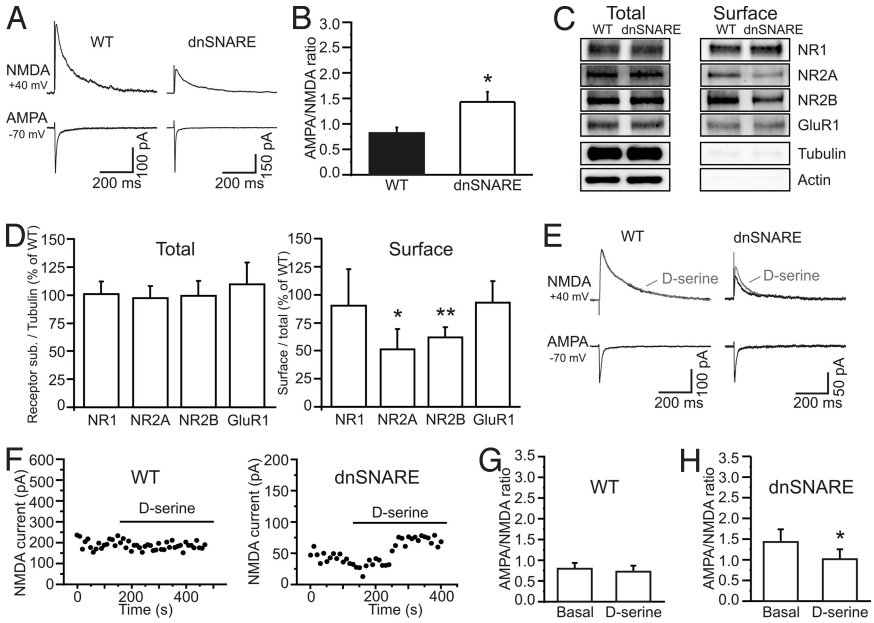

Fig. 3. Astrocytes control NMDA receptor activity at intracortical synapses. (*A*) Example of AMPA- and NMDA-mediated EPSCs in WT and dnSNARE animals. Traces are the average of at least 10 consecutive EPSCs. (*B*) Average AMPA/NMDA ratio in 13 cells from 4 WT and 14 cells from 4 dnSNARE animals. (*C*) Total (total, 1/10 of input) (*Left*) and cell surface (surface) (*Right*) protein from somatosensory cortical slices were immunoblotted with anti-NR1, NR2A, NR2B, GluR1, α-tubulin, and β-actin antibodies. (*D*) The expression of each subunit was normalized by tubulin (receptor/tubulin) and the immunoblots of dnSNARE mouse were compared with those in WT (NR1, NR2A, GluR1, $n = 5$; NR2B, $n = 6$ animals) (*Left*). The surface expression of each subunit was normalized by their total (surface/total), and the immunoblots from dnSNARE mice were compared with the WT ($n = 5$, *, $P < 0.05$, **, $P < 0.001$) (*Right*). (*E* and *F*) Representative examples of AMPA- and NMDA-mediated EPSCs (*E*) and time course of the NMDA-mediated currents (*F*) in WT and dnSNARE animals before and after application of D-serine (100 μM). Traces in *E* are the average of at least 10 consecutive EPSCs. (*G* and *H*) AMPA/NMDA ratio in nine cells from four WT and in eight cells from four dnSNARE animals under the different experimental conditions.

tions in control animals (Fig. 4 *A–C*) in agreement with previous studies (4, 11). NR2B-containing NMDA receptors have been shown to be an important target of glutamate release from astrocytes (26). Application of ifenprodil (10–15 μM; Fig. S6 *F* and *G*), an antagonist of the NR2B-containing NMDA receptors, had no effect on cortical slow oscillation power, suggesting that NR2B-containing receptors do not have a crucial role in the generation and maintenance of this rhythm.

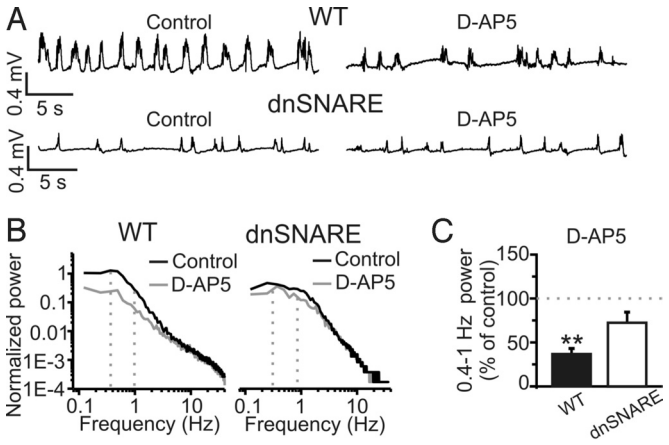

Fig. 4. Smaller contribution of NMDA receptors to slow oscillations in dnSNARE compared with WT mice. (*A*) Representative traces of LFP recordings from a WT (*Upper*) and a dnSNARE (*Lower*) animal showing the effect of D-AP5 (100 μM) on slow oscillations. (*B*) Power spectra of the experiments shown in *A*. (*C*) Mean values of the power of the slow oscillations in 13 WT and 11 dnSNARE animals in the presence of D-AP5 (50–100 μM). Values are expressed as percentage of slow oscillation power under control conditions (see *SI Materials and Methods*). Values of the power of the slow oscillations under basal conditions for WT and dnSNARE mice from this as well as for other pharmacological experiments were pooled together in Fig. 2*C*.

Because dnSNARE expression and NMDA receptor antagonists similarly reduce cortical slow oscillation power, we asked whether the inhibitory action of D-AP5 would be occluded by glial dnSNARE expression. In contrast to control animals, the addition of D-AP5 to dnSNARE mice did not significantly reduce the power of cortical slow oscillations (Fig. 4 *A–C*). Specificity of action of D-AP5 was confirmed by the observation that (5*S*,10*R*)-(+)-5-Methyl-10,11-dihydro-5H-dibenzo[a,d]cyclohepten- 5,10-imine maleate (MK-801; 20–40 μM), a different NMDA receptor antagonist, had a similar action in control mice (Fig. S7) with no significant effect in dnSNARE animals.

Given that dnSNARE expression in astrocytes reduces synaptic D-serine in brain slice preparation, we tested whether D-serine had a differential effect on cortical slow oscillations in WT and dnSNARE animals. Application of exogenous D-serine (300 μM) causes a significant increase in the power of these oscillations in dnSNARE animals (Fig. S8). The increase in cortical slow oscillation power in dnSNARE animals (163 $\pm$ 11% of control, $n = 9$) was significantly higher than the effect of D-serine in WT animals (131 $\pm$ 8% of control, $n = 10$; $P <$ 0.05) (Fig. S8*C*). Altogether these results are consistent with the notion that the reduced NMDA receptor function resulting from glial dnSNARE expression leads, at least in part, to the altered cortical slow oscillations observed in these transgenic mice in vivo.

Slow Oscillations Are Endogenously Modulated at Multiple Loci. Prior investigations using dnSNARE mice have demonstrated that astrocyte-derived adenosine causes a tonic A1 receptor-mediated inhibition of excitatory synaptic transmission (17, 20). Therefore, we took the opportunity afforded by the dnSNARE mouse to ask whether slow oscillations are endogenously mod-

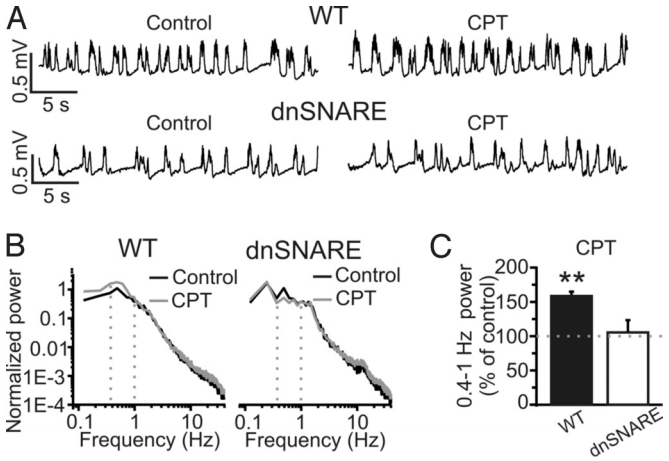

Fig. 5. The A1 receptor antagonist CPT increases slow oscillations in WT, but not in dnSNARE animals. (*A*) LFP Traces showing the effect of CPT on slow oscillations in WT (*Upper*) and dnSNARE (*Lower*) mice. (*B*) Power spectra of the experiments displayed in *A*. (*C*) Mean values of slow oscillation power after CPT (10 μM; WT, $n = 6$; dnSNARE, $n = 6$).

ulated at multiple loci, the A1 receptor as well as the NMDA receptor.

Topical application of the A1 receptor antagonist 8-cyclopentyl-1.3-dimethylxanthine (CPT; 10 μM) caused a significant increase in slow oscillation power in control animals (Fig. 5 *A–C*). In contrast, application of CPT had no effect on slow oscillation power in dnSNARE mice (Fig. 5 *A–C*). Decreasing CPT concentration to 1 μM had a similar effect (WT, 137 ± 11% of control, $n = 10$, $P < 0.01$; dnSNARE, 113 ± 16% of control, $n = 8$, $P > 0.05$). These results agree with experiments performed in cortical slices showing that astrocytes provide a tonic activation of A1 receptors that inhibits cortical excitatory synapses (20). Application (20–30 min) of the A1 receptor agonist 2-Chloro-N-cyclopentyladenosine (CCPA; 10 μM) in dnSNARE animals leads to significant decrease in the power of the slow oscillations (basal 0.49 ± 0.02; CCPA, 0.13 ± 0.05; $n = 5$, $P < 0.01$), demonstrating that A1 receptors are expressed and functional in dnSNARE animals.

If astrocytic dnSNARE expression leads to two opposing effects on cortical slow oscillations (an hypofunction of synaptic NMDA receptors and a decreased activation of A1 receptors), the simultaneous pharmacological inhibition of NMDA and A1 receptors should decrease slow oscillations in WT mice similarly to what observed in dnSNARE animals. Indeed, coapplication of D-AP5 (50–100 μM) and CPT (1 μM) in WT animals caused a significant reduction of slow oscillations (Fig. S9).

Discussion

During NREM sleep and some forms of anesthesia, slow oscillations are the major cortical rhythm. In this study, we gained two fundamental insights into the regulation of these oscillations. First, that by releasing chemical transmitters, nonneuronal cells modulate slow oscillations. And second, that diverse signals converge on distinct receptors (A_1 and NMDA) to coordinately regulate network activity.

Selective Inhibition of Gliotransmission Results in Altered Network Activity in Vivo. Astrocytic dnSNARE expression reduces the power of slow oscillations under conditions of high sleep pressure in behaving mice. Under urethane anesthesia, a condition that promotes cortical slow oscillations, independent whole-cell and LFP recordings confirm a significant impact of gliotransmission on cortical slow oscillations. Our results are consistent with the idea that astrocytes continuously and dynamically regulate neuronal networks.

Our genetic manipulation is specific for astrocytes, because dnSNARE has never been detected in neurons, microglia, oligodendrocytes, or in $NG2^+$ glia in various brain regions (Fig. S1) (17, 19, 20). The modification of cortical slow oscillations is not due to developmental effects, because we limited transgene expression to a brief period in adult life (see *Materials and Methods*). Also, our observations are not the result of transgene insertion site, because we found indistinguishable results (see *Results*) within our control group from WT littermates and dnSNARE mice in which transgene expression was inhibited throughout life as a result of a dox-containing diet. Last, the depth of anesthesia was the same in WT and dnSNARE animals (see *Materials and Methods*). Most importantly, under conditions of high homeostatic pressure when slow oscillations are the main cortical activity, reduced EEG power in the frequency band corresponding to the slow oscillations was confirmed in behaving mice (Fig. 1), ruling out any potential effect of anesthesia in the observed phenomenon.

Astrocytes Modulate Slow Oscillations by Regulating Cortical Synapses at Multiple Sites. The changes we observed in cortical slow oscillations result from changes in synaptic receptor function. Dominant negative SNARE expression causes an hypofunction of postsynaptic NMDA receptors leading to an increased AMPA/NMDA ratio. Also, A1 receptors are well known for causing powerful suppression of synaptic transmission (20, 30, 31). Indeed, in the hippocampus and cortex, the expression of dnSNARE in astrocytes leads to an enhancement of synaptic transmission that results from reduced extracellular adenosine and the consequent removal of a tonic A1-mediated inhibition (17, 20). The effects that we observe on cortical slow oscillations in the dnSNARE mice are likely to be generated by the integration of multiple effects on A1 and NMDA receptors at cortical synapses as confirmed by the finding that simultaneous inhibition of the NMDA and A1 receptors results, in WT mice, in a reduction of slow oscillation power similar to that observed in dnSNARE animals (Fig. S9).

It is important to note that the increase in AMPA/NMDA ratio at cortical synapses and the consequent shortening of up-state duration of cortical neurons during slow oscillations agrees with computational models showing that AMPA/NMDA ratio is crucial in shaping the transition to the depolarized phase of the slow oscillations (32).

In conclusion, we show that a nonneuronal cell, the astrocyte, modulates cortical rhythms by regulating synaptic receptor function, which is expected to lead to important changes in synaptic transmission. Astrocytic modulatory actions on cortical synapses involve multiple pathways. On the one hand, astrocytes exert an excitatory action on synaptic transmission by regulating NMDA receptors. On the other, they tonically suppress synapses through A1 receptors. These data demonstrate that certain brain oscillations are generated by the combined action of neuronal and glial networks in which synaptic connectivity generates the rhythm that is modulated by astrocyte-dependent synaptic regulation.

Materials and Methods

In Vivo EEG/EMG Recordings. All procedures were in strict accordance with the National Institutes of Health Guide for the Care and Use of Laboratory Animals and were approved by the Tufts University, University of Pennsylvania Institutional Animal Care and Use Committees, and the Italian Ministry of Health. EEG/EMG implantation surgery was performed as in ref. 33. EEG/EMG signals were conveyed by a light-weight cable, high- and low-pass filtered at 0.3 and 30 Hz and 10 and 100 Hz, respectively (15 LT Bipolar amplifier; Astro-Med), amplified and sampled at 200 Hz. Description of EEG data analysis can be found in the *SI Materials and Methods*.

In Vivo Patch-Clamp Recordings. Bigenic GFAP.tTA and tetO.dnSNARE transgenic animals (dnSNARE mice) (17) and their WT littermates aged 6–12 weeks old were anesthetized by an intraperitoneal injection of urethane (2 g/kg). Because these transgenic mice have been backcrossed onto a C57BL6/J genotype for >10 generations, C57BL6/J mice were used as controls in some experiments. Because no difference was observed between C57BL6/J and the WT littermates of dnSNARE mice, control data were pooled. Body temperature was measured with a rectal probe and kept at 37 °C with a heating pad. Depth of anesthesia was assured by continuously monitoring, respiration rate, eyelid reflex, vibrissae movements, and monitoring reactions to tail and toe pinching. Monitoring all these parameters no difference in anesthesia depth was observed between WT and dnSNARE animals. After the animal was anesthetized, an incision was made and the skull exposed. A craniotomy (1.8 mm) was drilled in the skull overlaying the somatosensory cortex, and the surface of the cortex was continuously kept moist with normal Hepes-buffered artificial cerebrospinal fluid (aCSF). The dura was carefully dissected, and a metal plate was glued on the skull for head fixation. Patch-clamp recordings were performed as described in ref. 34; 3- to 4-MΩ glass pipette were used as recording electrodes and filled with the following intrapipette solution (in mM): K-gluconate 140, $MgCl_2$ 1, NaCl 8, Na_2ATP 2, NaGTP 0.5, Hepes 10, phophocreatine 10 to pH 7.2 with KOH. Biocytin 2 mg/mL was included in the pipette solution for subsequent morphological reconstruction. Signals were amplified by a Multiclamp 700 B, filtered at 2 KHz, digitized at 10 KHz with a digidata 1320, and stored with pClamp 9.2 (Axon instruments). Details on data analysis and slice electrophysiology can be found in *SI Materials and Methods*.

In Vivo Extracellular Recordings. Mouse preparation and surgery was as described for patch-clamp experiments. LFPs were recorded with custom-built electrodes made of two parallel tungsten electrodes (FHC). Electrodes were placed to record from the superficial layers of the somatosensory cortex. Signals were amplified with an AM-amplifier (AM-system), filtered at 0.1 Hz-10 KHz, and digitized at 50 KHz. Recordings started 5–10 min after the electrodes were inserted in the cortex. For the description of data analysis, see *SI Materials and Methods*.

Statistics. In in vivo experiments, *N* values always refer to animal number, whereas in slice experiments, *N* values refer to the slice number. Student's *t* test was generally used to evaluate statistical significance. In pharmacological experiments when drug effect was assessed within the same animal, paired *t* test was used. For Fig. S3*C*, Kolmogorov–Smirnov test was used. Data are presented as mean ± SEM. A 2-factor ANOVA (frequency, genotype) was used to compare the power spectra in Fig. 1.

ACKNOWLEDGMENTS. We thank Dr. D. Contreras and Dr. M. B. Dalva for comments. This work was supported by National Institutes of Health and the Italian Institute of Technology.

1. Steriade M (2006) Grouping of brain rhythms in corticothalamic systems. *Neuroscience* 137:1087–1106.
2. Steriade M, Nunez A, Amzica F (1993) Intracellular analysis of relations between the slow (less-than-1 Hz) neocortical oscillation and other sleep rhythms of the electroencephalogram. *J Neurosci* 13:3266–3283.
3. Steriade M, Contreras D, Dossi RC, Nunez A (1993) The slow (less-than-1 Hz) oscillation in reticular thalamic and thalamocortical neurons: Scenario of sleep rhythm generation in interacting thalamic and neocortical networks. *J Neurosci* 13:3284–3299.
4. Steriade M, Nunez A, Amzica F (1993) A novel slow (less-than-1 Hz) oscillation of neocortical neurons in-vivo: Depolarizing and hyperpolarizing components. *J Neurosci* 13:3252–3265.
5. Petersen CCH, Hahn TTG, Mehta M, Grinvald A, Sakmann B (2003) Interaction of sensory responses with spontaneous depolarization in layer 2/3 barrel cortex. *Proc Natl Acad Sci USA* 100:13638–13643.
6. Huber R, Ghilardi MF, Massimini M, Tononi G (2004) Local sleep and learning. *Nature* 430:78–81.
7. Marshall L, Helgadottir H, Molle M, Born J (2006) Boosting slow oscillations during sleep potentiates memory. *Nature* 444:610–613.
8. Shu YS, Hasenstaub A, McCormick DA (2003) Turning on and off recurrent balanced cortical activity. *Nature* 423:288–293.
9. Amzica F, Steriade M (1995) Disconnection of intracortical synaptic linkages disrupts synchronization of a slow oscillation. *J Neurosci* 15:4658–4677.
10. Cunningham MO, et al. (2006) Neuronal metabolism governs cortical network response state. *Proc Natl Acad Sci USA* 103:5597–5601.
11. Compte A, Sanchez-Vives MV, McCormick DA, Wang XJ (2003) Cellular and network mechanisms of slow oscillatory activity (< 1 Hz) and wave propagations in a cortical network model. *J Neurophysiol* 89:2707–2725.
12. Newman EA (2003) New roles for astrocytes: Regulation of synaptic transmission. *Trends Neurosci* 26:536–542.
13. Volterra A, Meldolesi J (2005) Astrocytes, from brain glue to communication elements: The revolution continues. *Nat Rev Neurosci* 6:626–640.
14. Martineau M, Baux G, Mothet JP (2006) D-serine signalling in the brain: Friend and foe. *Trends Neurosci* 29:481–491.
15. Panatier A, et al. (2006) Glia-derived D-serine controls NMDA receptor activity and synaptic memory. *Cell* 125:775–784.
16. Zhang JM, et al. (2003) ATP released by astrocytes mediates glutamatergic activity-dependent heterosynaptic suppression. *Neuron* 40:971–982.
17. Pascual O, et al. (2005) Astrocytic purinergic signaling coordinates synaptic networks. *Science* 310:113–116.
18. Ventura R, Harris KM (1999) Three-dimensional relationships between hippocampal synapses and astrocytes. *J Neurosci* 19:6897–6906.
19. Halassa MM, Fellin T, Takase H, Dong JH, Haydon PG (2007) Synaptic islands defined by the territory of a single astrocyte. *J Neurosci* 27:6473–6477.
20. Halassa MM, et al. (2009) Astrocytic adenosine controls sleep homeostasis and cognitive consequences of sleep loss. *Neuron* 61:213–219.
21. Zhang Q, et al. (2004) Fusion-related release of glutamate from astrocytes. *J Biol Chem* 279:12724–12733.
22. Orthmann-Murphy JL, Enriquez AD, Abrams CK, Scherer SS (2007) Loss-of-function GJA12/Connexin47 mutations cause Pelizaeus-Merzbacher-like disease. *Mol Cell Neurosci* 34:629–641.
23. Matthias K, et al. (2003) Segregated expression of AMPA-type glutamate receptors and glutamate transporters defines distinct astrocyte populations in the mouse hippocampus. *J Neurosci* 23:1750–1758.
24. Bergles DE, Jahr CE (1997) Synaptic activation of glutamate transporters in hippocampal astrocytes. *Neuron* 19:1297–1308.
25. Saint Jan DD, Westbrook GL (2005) Detecting activity in olfactory bulb glomeruli with astrocyte recording. *J Neurosci* 25:2917–2924.
26. Fellin T, et al. (2004) Neuronal synchrony mediated by astrocytic glutamate through activation of extrasynaptic NMDA receptors. *Neuron* 43:729–743.
27. Timofeev I, Grenier F, Bazhenov M, Sejnowski TJ, Steriade M (2000) Origin of slow cortical oscillations in deafferented cortical slabs. *Cerebral Cortex* 10:1185–1199.
28. Sanchez-Vives MV, McCormick DA (2000) Cellular and network mechanisms of rhythmic recurrent activity in neocortex. *Nat Neurosci* 3:1027–1034.
29. Mothet JP, et al. (2005) Glutamate receptor activation triggers a calcium-dependent and SNARE protein-dependent release of the gliotransmitter D-serine. *Proc Natl Acad Sci USA* 102:5606–5611.
30. Brand A, Vissiennon Z, Eschke D, Nieber K (2001) Adenosine A(1) and A(3) receptors mediate inhibition of synaptic transmission in rat cortical neurons. *Neuropharmacology* 40:85–95.
31. Lopes LV, Cunha RA, Ribeiro JA (1999) Cross-talk between A(1)/A(2A) adenosine receptors in the rat hippocampus and cortex. *Br J Pharmacol* 127:U20.
32. Wolf JA, et al. (2005) NMDA/AMPA ratio impacts state transitions and entrainment to oscillations in a computational model of the nucleus accumbens medium spiny projection neuron. *J Neurosci* 25:9080–9095.
33. Frank MG, Stryker MP, Tecott LH (2002) Sleep and sleep homeostasis in mice lacking the 5-HT2c receptor. *Neuropsychopharmacology* 27:869–873.
34. Margrie TW, Brecht M, Sakmann B (2002) In vivo, low-resistance, whole-cell recordings from neurons in the anaesthetized and awake mammalian brain. *Pflug Arch Eur J Phy* 444:491–498.